Use of Static Magnetic Fields for Multipactor Mitigation in Coaxial Transmission Lines

D. González-Iglesias[1], A. M. Perez[1], S. Anza[2], J. Vague[3],

B. Gimeno[1], V. E. Boria[3], D. Raboso[4], C. Vicente[2], J. Gil[2], L. Conde[5],

[1]Depto. Física Aplicada y Electromagnetismo – ICMUV, Universidad de Valencia, Valencia [2] AURORASAT, Valencia

[3] Depto. Comunicaciones – iTEAM, Universidad Politécnica de Valencia, Valencia [4] Agencia Espacial Europea, ESA/ESTEC, Noordwijk, Holland

[5] Department of Applied Physics, Faculty of Aeronautics Engineers, Technical University of Madrid, Spain

1. Introduction

Multipactor breakdown is a phenomenon that takes place on devices operating under vacuum conditions and high power RF electromagnetic fields [1]. The discharge occurs when the trajectories of free electrons, existing inside the device, are synchronized with the RF electric field, producing an exponential growth of the electron population and generating several negative effects which degrade the device performance.

The main aim of this work is the analysis of the mitigation of a multipactor discharge existing within a coaxial waveguide structure by means of the use of a DC magnetic field. In a first step, it is studied the case of an uniform axial DC magnetic field, which is achieved by placing the coaxial sample within a solenoid. In a second step, it is analyzed the case of an non uniform axial and radial DC magnetic field, which is provided by a hollow cylindrical magnet.

2. Theory

The commercial FEST3D software [2] was used to perform the multipactor simulations within the coaxial line, for the axial DC uniform magnetic field case. However, for the axial and radial non uniform DC magnetic field case, an in-house code had to be developed to consider the field generated by the magnet. Both multipactor simulation algorithms are based on the 3-D tracking of a set of electrons governed by electric and magnetic external fields. To proceed, the Lorentz force equation is numerically solved. Following the Monte Carlo technique, when an electron hits on the inner or the outer metallic walls, the code allows absorbing the electron or releasing secondary electrons depending on the impact conditions. This is done by using the secondary-electron-yield coefficient δ (SEY) [3] of the material.

3. Uniform axial DC magnetic field: Solenoid

An external axial DC magnetic field is applied to the coaxial (see Fig. 1) sample by means of a long solenoid, with dimensions selected to ensure a uniform magnetic field in the central region, where the coaxial sample is inserted.

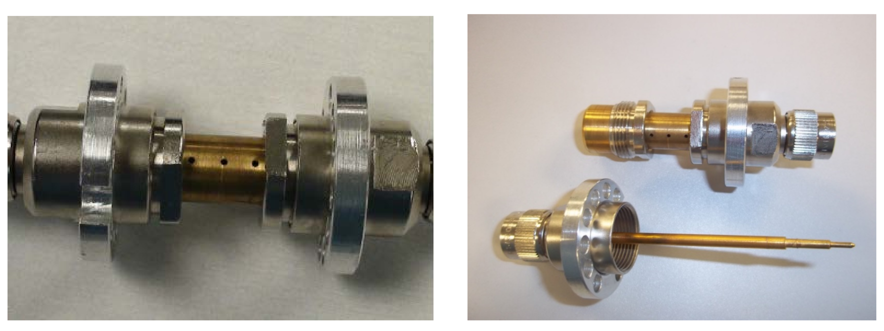

Fig. 1. Picture of the coaxial sample assembled (left) and disassembled (right).

The solenoid was calibrated by means of the electromagnetic induction phenomenon, using a magnetic probe mounted in a translation linear stage (see Fig. 2), which moves along the axis of symmetry of the solenoid. In the center of the solenoid the magnetic field is 3.8 mT when it is fed by a DC electric current of 100 mA.

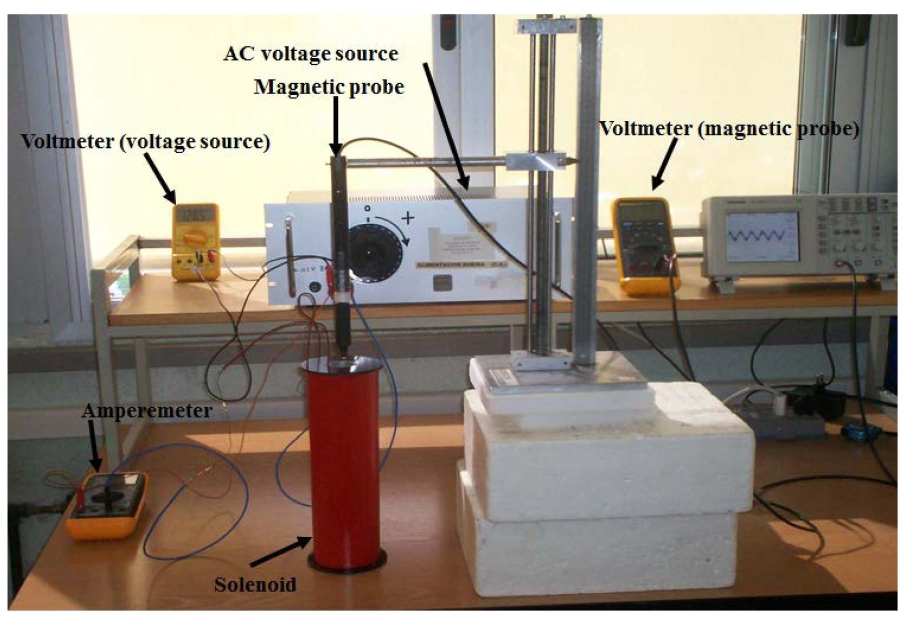

Fig. 2. Solenoid calibration set-up with the magnetic probe mounted in the translation linear stage.

Multipactor measurements were performed for the RF frequencies of f = 1.145 GHz and f = 0.435 GHz. Multipactor RF power threshold was measured for several DC magnetic field strengths. Both experimental and theoretical results (FEST3D) are shown in Fig. 3.

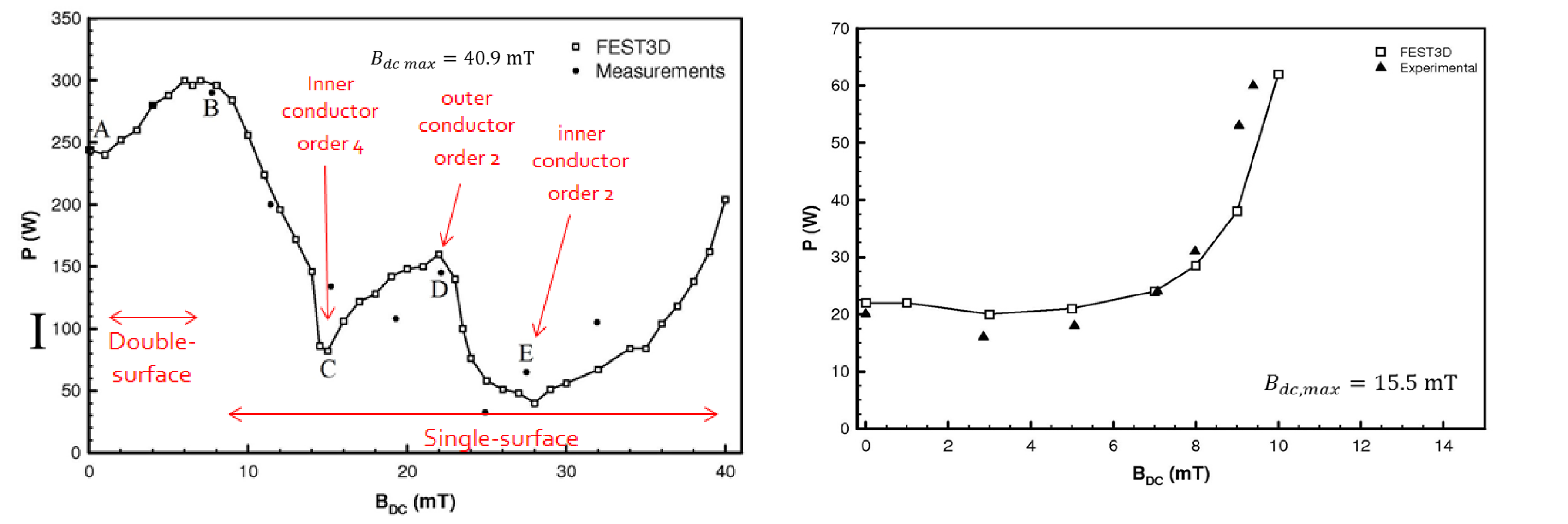

Fig. 3. Multipactor RF power threshold as a function of the DC magnetic field strength (left: f = 1.145 GHz, right: f = 0.435 GHz). Experimental and theoretical results are shown.

In view of the results from Fig. 3, there is good agreement between theoretical simulations and experimental data. Multipactor discharge is suppressed when the cyclotron frequency ($f_c = \frac{1}{2\pi}\frac{e}{m}B_{DC}$) exceeds the RF frequency value. According to this statement, in Fig. 3 it is shown the theoretical maximum value at which the discharge is present, $B_{dc,\ max}$. For a better understanding of the multipactor phenomenon, in Fig. 4 it is depicted the electron trajectories for some relevant points of the Fig. 3.

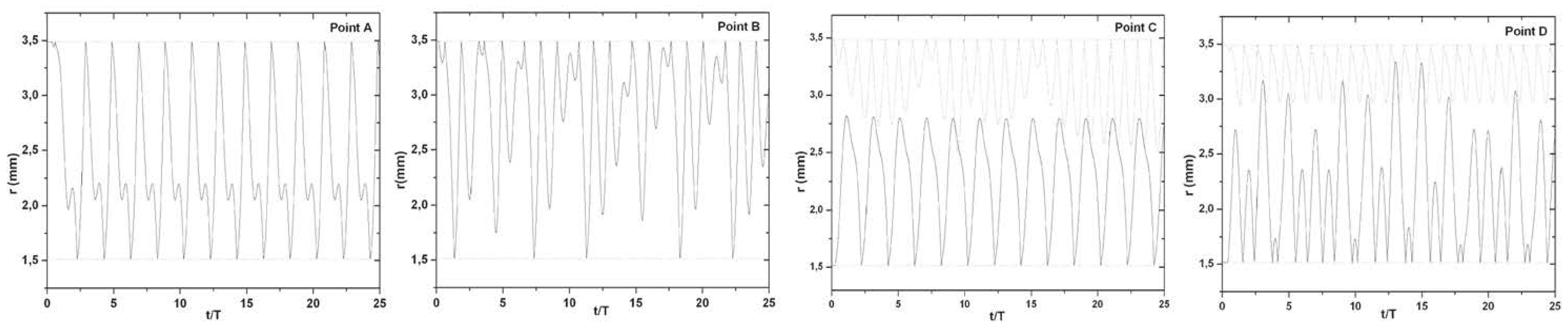

Fig. 4. Electron trajectories of the points A, B, C and D of Fig. 3. Cylindrical radial coordinate of the effective electron *r* has been plotted as a function of the normalized time t/T, T being the RF period (T=1/f).

4. Axial and radial non uniform DC magnetic field: Magnet

A hollow cylindrical neodymium magnet has been designed and manufactured (see Fig. 5, right). Theoretical simulations and experimental measurements for the multipactor RF power threshold as a function of the RF frequency gap are shown in Fig. 5 (center). With magnet and without magnet configurations are explored, demonstrating the feasibility of the magnet prototype to suppress the multipactor discharge.

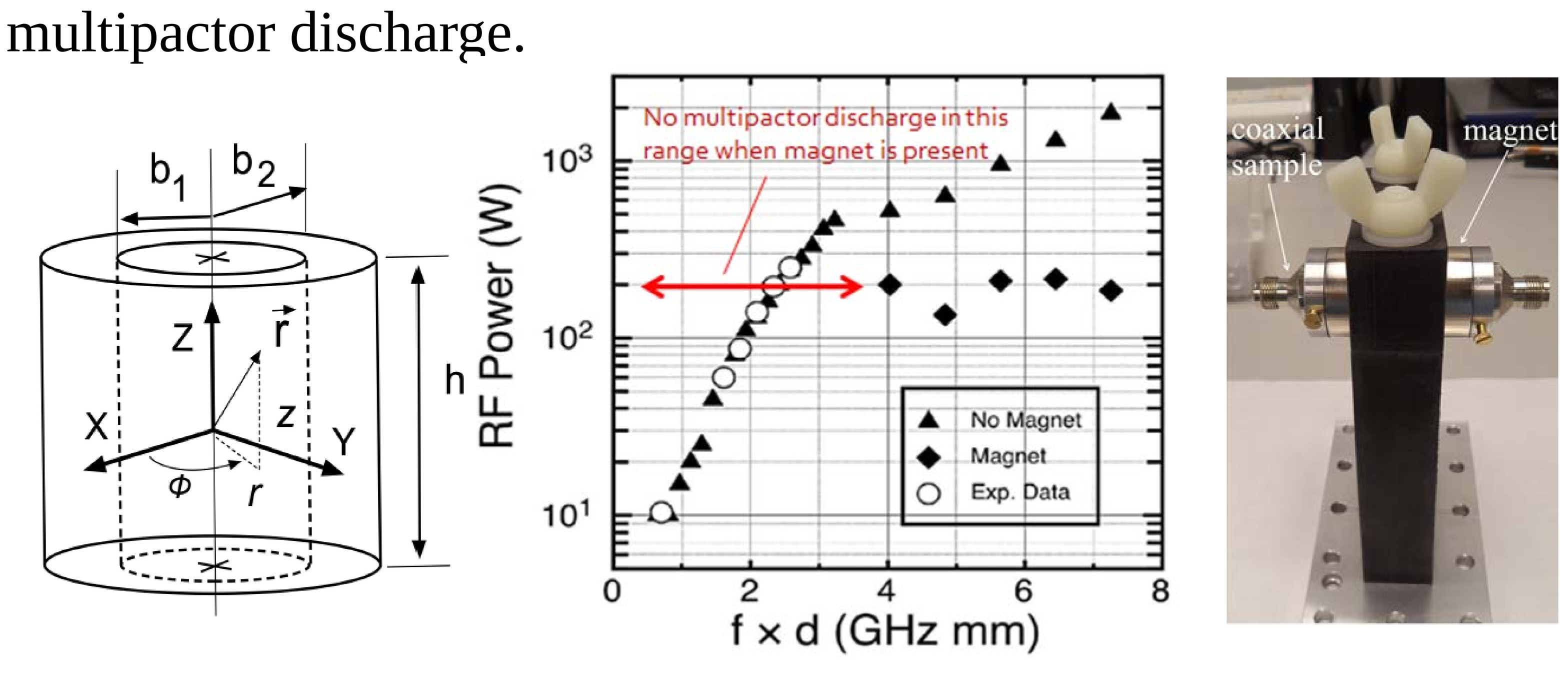

Fig. 5. Right: scheme of the hollow magnet with height *h*, and b_1 and b_2 radii. Center: comparison of numerical calculations (solid symbols) with the experimental data (open symbols) without external magnetic field. The RF power thresholds are represented against the frequency gap (gap remains fixed). Note that multipactor discharge was not experimentally detected in the presence of the permanent magnet in the explored frequency range. Left: coaxial sample inserted in the hollow coaxial magnet.

5. References

[1] J. Vaughan, "Multipactor", *IEEE Trans. Electron Devices*, vol. 35, no. 7, pp. 1172-1180, July 1988.

[2] FEST3D, ESA/ESTEC, Valencia, Spain, [Online]. Available: www.fest3d.com

[3] S. Anza, C. Vicente, D. Raboso, J. Gil, B. Gimeno, V. E. Boria, "Enhanced Prediction of Multipaction Breakdown in Passive Waveguide Components including Space Charge Effects", Microwave Symp. Digest, 2008 IEEE MTT-S pp. 1095-1098.